To appear in Journal of Applied Mechanics

Division of Engineering
BROWN UNIVERSITY
PROVIDENCE, R. I.

THE PART-THROUGH SURFACE CRACK IN AN ELASTIC PLATE

J. R. RICE and N. LEVY

Technical Report NASA NGL 40-002-080/3 to the National Aeronautics and Space Administration

September 1970

Rat-65327

The Part-Through Surface Crack in an Elastic Plate

by J. R. Rice* and N. Levy**

Division of Engineering, Brown University, Providence, R. I.

September 1970

Technical Report NGL 40-002-080/3 to the National Aeronautics and Space Administration

* Professor of Engineering

** Research Associate

Abstract

An elastic analysis is presented for the tensile stretching and bending of a plate containing a surface crack penetrating part through the thickness (fig. 1). The treatment is approximate, in that the two-dimensional generalized plane stress and Kirchhoff-Poisson plate bending theories are employed, with the part-through cracked section represented as a continuous line spring. The spring has both stretching and bending resistance, its compliance coefficients being chosen to match those of an edge cracked strip in plane strain. The mathematical formulation reduces finally to two coupled integral equations for the thickness averaged force and moment per unit length along the cracked section. These are solved numerically for the case of a semi-elliptical part-through crack, with results compared to a simple but approximate closed-form solution. Extensive results are given for the stress intensity factor at the midpoint of the part-through crack for both remote tensile and bending loads on the plate. These results indicate significant load shedding to uncracked regions of the plate, in that the stress intensity factor is substantially lower (in general) than for a similarly loaded strip in plane strain with a crack of the same depth.

Introduction

Fig. 1 shows the configuration studied here. An elastic plate of thickness h, and of infinite planar extent, contains a surface crack penetrating part through the thickness. At remote distances from the crack site, the plate is subjected to loads equipollent to a uniform simple tension in the x_2 direction and to pure bending about the x_1 direction. This configuration, and its variants for curved shells rather than plates, is of considerable interest in the fracture resistant design of pipelines, reactor vessels, pressurized fuel tanks, and other plate and shell structures.

An exact analysis for the elastic stress intensity factor along the crack front is precluded by the decidedly three dimensional nature of the problem. Thus an approximate analysis is developed here, which appears more nearly exact when the surface length of the crack (distance 2a in fig. 1) is large compared to the plate thickness. The approximation relies heavily on the known solution for an edge cracked strip in plane strain as in fig. 2, subjected to an axial force N and moment M per unit length in the direction of plane strain constraint. In particular we shall employ the exact expressions for the stress intensity factor and for the increase in compliance due to introduction of the crack, from the solution for the edge cracked strip in plane strain, as a basis for approximate analysis of the part through surface crack. Note that the plane strain configuration of fig. 2 corresponds to the configuration of fig. 1 in the special case for which the surface length 2a of the crack is infinite and the crack depth $\ell(x_1)$ is constant.

The following procedure is adopted:

Let $\tau_{ij}(x_1,x_2,x_3)$ be the stress state in the three dimensional body of fig. 1. Define

$$N_{22}(x_1,0) = \int_{-h/2}^{+h/2} \tau_{22}(x_1,0,x_3)dx_3 \quad , \quad \text{and}$$

$$M_{22}(x_1,0) = \int_{-h/2}^{+h/2} x_3\tau_{22}(x_1,0,x_3)dx_3 \qquad (1)$$

as the net force and moment, per unit length in the x_1 direction, which act on the plane $x_2 = 0$ containing the crack. For the approximation, we shall assume that the stress intensity factor at a point along the crack front with coordinate x_1 is identical to the stress intensity factor for an edge cracked strip in plane strain (fig. 2) subjected to an axial force and moment equal, respectively, to $N_{22}(x_1,0)$ and $M_{22}(x_1,0)$, and having a crack depth equal to $\ell(x_1)$. This method of approximating the stress intensity factor appears most appropriate along the central section of the crack shown in fig. 1, but much less appropriate near the ends where the crack intersects the free surface. Fortunately, the stress intensity factor along the central section, where breaking through to the far plate surface is imminent, is of considerable practical interest. Later, we shall discuss a more elegant method for approximating the stress intensity factor, based on its relation to the variation of potential energy with crack position, and show (via the Appendix) that the latter method leads to the same approximation as outlined above.

Thus, to determine the stress intensity factor at points along the crack tip, we must compute the force and moment transmitted across the cracked section.

We obtain these through the simple approximate theories of generalized plane stress and Kirchhoff-Poisson plate bending, employed in conjunction with a representation of the part through surface crack as a continuously distributed line spring with compliance coefficients chosen to match the compliance of an edge cracked strip in plane strain.

Specifically, the problem of fig. 1 is formulated as the two-dimensional problem of simultaneous plane stress and plate bending for an infinite sheet in the x_1, x_2 plane, subjected to remotely uniform stretching and bending loads, and containing a line discontinuity on the x_1 axis from $-a$ to $+a$, as shown in fig. 3. The line discontinuity represents a spring having both stretching and bending resistance. Let

$$\delta(x_1) = u_2^+(x_1,0) - u_2^-(x_1,0) \tag{2}$$

be the opening displacement along the line of discontinuity (+ and - signs referring as in fig. 3 to top and bottom limits along the discontinuity), and let

$$\theta(x_1) = \frac{\partial u_3^-(x_1,0)}{\partial x_2} - \frac{\partial u_3^+(x_1,0)}{\partial x_2} \tag{3}$$

be the angle of rotation of one side of the discontinuity relative to the other. (Here we use the two dimensional notation of plate theory, $u_1(x_1,x_2)$ and $u_2(x_1, x_2)$ being thickness averaged in-plane displacements, and $u_3(x_1, x_2)$ being the transverse displacement.) Both δ and θ are taken to be linear functions of the net force $N_{22}(x_1, 0)$ and moment $M_{22}(x_1, 0)$ transmitted across the line of discontinuity. We choose these

functional relations by returning to the two dimensional plane strain problem of fig. 2. For a given net force and moment on the strip, the presence of the crack will cause the displacement and rotation of one end relative to the other to increase over the values which would result in an uncracked strip. These increases are identified as δ and θ, and the exact functional relation to the net force and moment for the edge cracked strip is adopted for the line of discontinuity in fig. 3. Thus, we are lumping the increased compliance due to the crack into the continuously distributed spring. The spring constants will, of course, depend on x_1 since the crack depth $\ell(x_1)$ is variable. This relation of δ and θ to the force and moment provides the boundary condition along the discontinuity, and solution of the problem leads to expressions for the force and moment from which the stress intensity factor is calculated.

The details of calculation, outlined in the following sections, lead finally to two coupled integral equations for the net force and moment transmitted across the line of discontinuity. By virtue of a convenient approximation for the variation of spring constants with x_1, a solution of the integral equations is obtained which involves constant net force and moment. This solution compares rather favorably with exact solutions of the integral equations obtained by digital computation. Resulting values for the stress intensity factor in the central section of the crack are presented graphically for a range of parameters.

For notation, it turns out to be more convenient to use the thickness average stresses $\sigma_{\alpha\beta}$ and nominal bending stresses $m_{\alpha\beta}$, defined by

$$\left.\begin{aligned} \sigma_{\alpha\beta} &= \frac{N_{\alpha\beta}}{h} = \frac{1}{h}\int_{-h/2}^{+h/2} \tau_{\alpha\beta}\, dx_3 \\ m_{\alpha\beta} &= \frac{6\, M_{\alpha\beta}}{h^2} = \frac{6}{h^2}\int_{-h/2}^{+h/2} x_3 \tau_{\alpha\beta}\, dx_3 \end{aligned}\right\} \quad \alpha,\beta = 1,2 \qquad (4)$$

Thus, for example, fig. 2 shows the remote loads on the edge cracked strip in terms of σ and m, and the remotely applied loads on the configurations of figs. (1) and (3) are denoted by σ_∞ and m_∞.

Note that two approximations are involved in the procedure outlined above: The stress intensity factor is calculated from $N_{22}(x_1, 0)$ and $M_{22}(x_1, 0)$, according to the exact expression for the edge cracked strip in plane strain. The force and moment are calculated from two dimensional plane stress-plate bending theory, with the cracked section represented as a continuous line spring having compliance matched to that of the edge cracked strip in plane strain. One could equally well adopt only the second approximation, and compute from it the total potential energy of the system (i.e., strain energy of stretching and bending stress fields in the plate, plus energy of the line spring, plus potential energy of the load system) as a functional of crack depth. Then Irwin's [1] relation between the variation in potential energy, accompanying a variation in crack depth, and the stress intensity factor could be employed as a basis for calculating the stress intensity factor. It is shown in the Appendix that this method leads to the same expression for the stress intensity factor as does the first approximation indicated above. (The Appendix relies on notation introduced in the next two sections).

Edge Cracked Strip in Tension and Bending (Fig. 2)

For the plane strain problem of fig. 2, it is well known [1,2] that the near crack tip stress state in an isotropic linear elastic material has the singular form

$$\tau_{ij} \to Kr^{-1/2} f_{ij}(\omega) \ , \quad \text{as} \quad r \to 0 \ , \tag{5}$$

where K is Irwin's stress intensity factor and $f_{ij}(\omega)$ is a set of functions of the orientation angle, which are identical for all symmetrically loaded crack configurations. The functions are normalized so that $\tau_{22} \to K(2\pi r)^{-1/2}$ as $r \to 0$ on the ray $\omega = 0$.

By dimensional considerations, it is clear that for the tension and bending loading of fig. 2,

$$K = h^{1/2} [\sigma g_t + m g_b] \ , \tag{6}$$

where g_t and g_b are dimensionless functions of the crack depth to thickness ratio ℓ/h . From Koiter's [3] solution for an edge crack in a half plane, it is clear that

$$g_t = g_b = 1.12 \, (\pi \ell/h)^{1/2} \qquad \text{for} \quad \ell << h \ . \tag{7}$$

More generally, one may use the well-known boundary collocation solution by Gross and Srawley [4] to write

$$\begin{aligned} g_t &= \xi^{1/2}[1.99 - 0.41\xi + 18.70\xi^2 - 38.48\xi^3 + 53.85\xi^4] \\ g_b &= \xi^{1/2}[1.99 - 2.47\xi + 12.97\xi^2 - 23.17\xi^3 + 24.80\xi^4] \end{aligned} \tag{8}$$

where $\xi = \ell/h$ = crack depth to thickness ratio

These equations were originally presented as being for the range $0 < \xi < 0.7$. In the sequel, numerical results for the stress intensity factor at the center point of the configuration of fig. 1 will be presented in the form of a ratio of K to the stress intensity factor for an infinitely long crack ($a \to \infty$), of depth equal to that at the center point, and subjected to the same remote loading for ratios of maximum part-through crack depth to plate thickness ℓ_o/h in the range $0.1 \leq \ell_o/h \leq 0.7$.

Now, as in the last section, let δ and θ be the <u>additional</u> displacement and rotation of one end of the strip relative to the other, due to introduction of the crack. Since $h\delta$ is the generalized displacement associated with σ, and $h^2\theta/6$ the generalized displacement associated with m, we may write

$$h\delta = A_{tt}\sigma + A_{tb}m \quad , \qquad \frac{h^2\theta}{6} = A_{bt}\sigma + A_{bb}m \quad , \tag{9}$$

where $A_{tb} = A_{bt}$ by elastic reciprocity. The compliance coefficients $A_{\lambda\mu}$ depend only on ℓ and vanish when $\ell = 0$. It is straightforward to generalize Irwin's [1] relation between the potential energy release rate,

$$G = \frac{1 - \nu^2}{E} K^2 = h \frac{1 - \nu^2}{E} (g_t^2\sigma^2 + 2g_t g_b \sigma m + g_b^2 m^2) \quad , \tag{10}$$

and the rate of change of compliance with crack length to cases for which

there is more than one generalized force. For example, if only σ acted in fig. 2, and m was zero, we would have $h\delta = A_{tt}\sigma$ and, following Irwin,

$$G = \frac{1}{2}\sigma\frac{\partial}{\partial \ell}(h\delta) = \frac{1}{2}\sigma^2\frac{dA_{tt}}{d\ell} \qquad \text{when} \quad m = 0 \quad . \tag{11}$$

The proper generalization for combined tension and bending is

$$\begin{aligned} G &= \frac{1}{2}\left[\sigma\frac{\partial}{\partial \ell}(h\delta) + m\frac{\partial}{\partial \ell}\left(\frac{h^2\theta}{6}\right)\right] \\ &= \frac{1}{2}\left[\sigma\left(\frac{dA_{tt}}{d\ell}\sigma + \frac{dA_{tb}}{d\ell}m\right) + m\left(\frac{dA_{bt}}{d\ell}\sigma + \frac{dA_{bb}}{d\ell}m\right)\right] \end{aligned} \tag{12}$$

Now, if we equate common coefficients in the quadratic forms of eqs. (10) and (12), recalling that the compliance coefficients are symmetric, we can solve for $dA_{\lambda\mu}/d\ell$. After integrating, the equations for δ and θ may be put in the forms

$$\begin{aligned} \delta &= \frac{2(1-\nu^2)h}{E}(\alpha_{tt}\sigma + \alpha_{tb}m) \\ \theta &= \frac{12(1-\nu^2)}{E}(\alpha_{bt}\sigma + \alpha_{bb}m) \quad , \end{aligned} \tag{13}$$

where the α's are dimensionless compliance coefficients, depending on the crack depth to thickness ratio ℓ/h , and defined by

$$\alpha_{\lambda\mu} = \frac{1}{h}\int_0^{\ell} g_\lambda g_\mu d\ell \quad , \qquad \lambda,\mu = b,t \quad . \tag{14}$$

If we insert the series from eqs. (8), each compliance coefficient may be represented in the form

$$\alpha_{\lambda\mu} = \xi^2 \sum_{n=0}^{8} C_{\lambda\mu}^{(n)} \xi^n \quad ; \quad \lambda,\mu = b,t \quad ; \quad \xi = \ell/h \ , \qquad (15)$$

where the coefficients $C_{\lambda\mu}^{(n)}$ are listed in Table 1. Fig. 4a shows a plot of the stress intensity coefficients (g_t, g_b) introduced in eqs. (6,8), and fig. 4b shows the dimensionless compliance coefficients $(\alpha_{tt}, \alpha_{tb}, \alpha_{bb})$, all as functions of the crack depth to thickness ratio ℓ/h .

As noted earlier, we will employ eqs. (13) relating (δ,θ) to (σ,m) as a boundary condition along the line of discontinuity in fig. 3, which represents the part through crack of fig. 1.

Okamura et al. [5] have presented a similar calculation of the compliance increase due to a crack, in their treatment of the notched column under compression. They consider the notched column as equivalent to two unnotched columns joined together by a torsional spring, with the spring constant chosen to simulate the compliance increase due to the notch. This is, of course, similar to the use of the compliance calculation in the present analysis. However, they considered a compliance analogous to α_{bb} only, and have neglected the rotation induced by the axial load (i.e. the effect of α_{bt} in eqs. 13). Thus their results can apply only in cases for which the nominal bending stress overwhelms the average compressive stress.

Tension and Bending Stress Fields

It is well known that solutions to two dimensional problems in the approximate theories of generalized plane stress and Kirchhoff-Poisson plate bending may be represented in terms of analytic functions of $z = x_1 + ix_2$ [6,7] :

plane stress:

$$u_1 + iu_2 = \frac{1+\nu}{E}\left[\frac{3-\nu}{1+\nu}\,\phi_t(z) - z\,\overline{\phi_t'(z)} - \overline{\psi_t(z)}\right]$$

$$\frac{\sigma_{11}+\sigma_{22}}{2} = \phi_t'(z) + \overline{\phi_t'(z)} \qquad (16)$$

$$\frac{\sigma_{22}-\sigma_{11}}{2} + i\,\sigma_{12} = \bar{z}\phi_t''(z) + \psi_t'(z)$$

plate bending:

$$\frac{\partial u_3}{\partial x_1} + i\,\frac{\partial u_3}{\partial x_2} = \phi_b(z) + z\,\overline{\phi_b'(z)} + \overline{\psi_b(z)}$$

$$\frac{m_{11}+m_{22}}{2} = -\frac{Eh}{2(1-\nu)}\left[\phi_b'(z) + \overline{\phi_b'(z)}\right] \qquad (17)$$

$$\frac{m_{22}-m_{11}}{2} + i\,m_{12} = \frac{Eh}{2(1+\nu)}\left[\bar{z}\phi_b''(z) + \psi_b'(z)\right]$$

$$V_1 - i\,V_2 = -\frac{Eh^3}{3(1-\nu^2)}\,\phi_b''(z)$$

Here $\phi_t(z)$, $\psi_t(z)$ and $\phi_b(z)$, $\psi_b(z)$ are analytic functions of z, and the bar over a quantity denotes the complex conjugate. Also, the transverse shears V_α are defined as the integral of $\tau_{3\alpha}$ across the thickness.

In our problem (fig. 3), the tension and bending fields are coupled by the boundary conditions along the line of discontinuity, which relate δ and θ to the values of σ_{22} and m_{22} transmitted across the discontinuity. We shall impose these conditions shortly, after separately constructing tension and bending solutions in terms of the as yet unknown stresses

$$\sigma(x_1) = \sigma_{22}(x_1, 0) \quad , \qquad m(x_1) = m_{22}(x_1, 0) \tag{18}$$

acting on the discontinuity.

For the tension problem, the vanishing of σ_{12} along the x_1 axis (by symmetry) and loading conditions at ∞ require

$$\psi_t'(z) = \frac{\sigma_\infty}{2} - z\phi_t''(z) \quad . \tag{19}$$

Following Muskelishvili [6], we may then show that conditions along the line of discontinuity are

$$[\phi_t'(x_1)]^+ + [\phi_t'(x_1)]^- = \sigma(x_1) - \frac{\sigma_\infty}{2} \quad , \qquad -a < x_1 < +a \quad . \tag{20}$$

The solution, resulting in the proper stress state at ∞ and in single valued displacements, is

$$\phi_t'(z) = -\frac{\sigma_\infty}{4} + \frac{\sigma_\infty}{2}\, z\,(z^2 - a^2)^{-1/2}$$

$$+ \frac{1}{2\pi}(z^2 - a^2)^{-1/2} \int_{-a}^{+a} \frac{\sigma(t)\sqrt{a^2 - t^2}\, dt}{t - z} \tag{21}$$

(Here the inverse square root function has its branch cut on the discontinuity, and behaves as z^{-1} for large z).

Similarly, for the bending problem, vanishing of the Kirchhoff shear

$$V_2 + \frac{h^2}{6} \frac{\partial m_{12}}{\partial x_1}$$

along the x_1 axis (by symmetry) and loading conditions at ∞ require

$$\psi_b'(z) = -\frac{1-\nu}{Eh} m_\infty - z\phi_b''(z) - \frac{4}{1-\nu}\phi_b'(z) \quad . \tag{22}$$

Along the line of discontinuity,

$$[\phi_b'(x_1)]^+ + [\phi_b'(x_1)]^- = -\frac{2(1-\nu^2)}{(3+\nu)Eh}\left[m(x_1) + \frac{1-\nu}{2(1+\nu)} m_\infty\right] \quad . \tag{23}$$

The solution, consistent with conditions at ∞ and single valued plate deflection, is

$$-\frac{(3+\nu)Eh}{2(1-\nu^2)}\phi_b'(z) = \frac{(1-\nu)m_\infty}{4(1+\nu)} + \frac{m_\infty}{2} z(z^2-a^2)^{-1/2}$$

$$+ \frac{1}{2\pi}(z^2-a^2)^{-1/2}\int_{-a}^{+a} \frac{m(t)\sqrt{a^2-t^2}\,dt}{t-z} \tag{24}$$

To impose boundary conditions in the form of eqs. (13) along the discontinuity, we must first solve for δ and θ as defined by eqs. (2,3). If ϕ_t and ϕ_b are both chosen to vanish at $z = -a$, then one may show from eqs. (16,17) and those above that

$$\delta(x_1) = \frac{8}{E}\,\mathrm{Im}[\phi_t^+(x_1)] \quad ; \qquad \theta(x_1) = -\frac{8}{1-\nu}\,\mathrm{Im}[\phi_b^+(x_1)] \quad . \tag{25}$$

To obtain ϕ_t and ϕ_b from eqs. (21,24), one needs a result of the form

$$\int_{-a}^{z} \frac{dz}{(z^2-a^2)^{1/2}(t-z)} = -\frac{i}{\sqrt{a^2-t^2}} \log\left[\frac{a^2 - zt - i(z^2-a^2)^{1/2}\sqrt{a^2-t^2}}{a(t-z)}\right] \tag{26}$$

Let us introduce the dimensionless variables

$$X = x_1/a \quad , \qquad T = t/a \quad , \tag{27}$$

and write $\delta(X)$ for $\delta(x_1)$, $m(T)$ for $m(t)$, etc. Then, employing eqs. (25) with Eq. (26), the opening δ and rotation θ along the line of discontinuity are

$$\frac{E\,\delta(X)}{4\,a} = \sigma_\infty \sqrt{1 - X^2} - \int_{-1}^{+1} G(X,T)\sigma(T)dT \quad , \tag{28}$$

$$\frac{(3 + \nu)Eh\theta(X)}{8(1 + \nu)a} = m_\infty \sqrt{1 - X^2} - \int_{-1}^{+1} G(X,T)m(T)dT \quad .$$

Here, the weight function is

$$G(X,T) = \frac{1}{\pi} \log \left[\frac{1 - TX + \sqrt{1 - X^2}\sqrt{1 - T^2}}{|T - X|} \right] , \tag{29}$$

and apart from multiplicative factors, this is the opening displacement (rotation) at X due to a point in-plane force (moment) at T . Note that G is symmetric in X and T .

Integral Equations Along Discontinuity; Variational Principle

We insist that the separation and relative rotation along the discontinuity be related to the tension and bending there by eqs. (13). When inserted into the equations above, the resulting integral equations for σ and m , to be solved in the range $|X| < 1$, are

$$\frac{1-\nu^2}{2}\,\frac{h}{a}\,[\alpha_{tt}(X)\sigma(X) + \alpha_{tb}(X)m(X)] + \int_{-1}^{+1} G(X,T)\sigma(T)dT = \sigma_\infty\sqrt{1-X^2}$$

$$\frac{3(3+\nu)(1-\nu)}{2}\,\frac{h}{a}\,[\alpha_{bt}(X)\sigma(X) + \alpha_{bb}(X)m(X)] + \int_{-1}^{+1} G(X,T)m(T)dT = m_\infty\sqrt{1-X^2} \qquad (30)$$

Note that the compliance coefficients $\alpha_{\lambda\mu}$ as defined by eqs. (14,15) are functions of the crack depth to thickness ratio ℓ/h. Since ℓ is some prescribed function of x_1, we adopt the notation $\alpha_{\lambda\mu}(X)$, although it should be remembered that these functions will also have a quantity such as $\ell(0)/h$ as a parameter. Once σ and m are determined from the integral equations, the stress intensity factor at points along the crack tip is given by eq. (6).

It may be readily shown that the integral equations are equivalent to the following variational principle: The functional $\Omega[\sigma(X), m(X)]$ is minimized by the functions $\sigma(X)$ and $m(X)$ constituting a solution of the problem, or $\Delta\Omega[\sigma(X), m(X)] = 0$ to first order for arbitrary variations $\Delta\sigma(X)$ and $\Delta m(X)$ from the correct solution, where

$$\Omega = \frac{1}{2}\int_{-1}^{+1}[\alpha_{tt}(X)\sigma^2(X) + 2\alpha_{tb}(X)\sigma(X)m(X) + \alpha_{bb}(X)m^2(X)]dX$$

$$+ \frac{2\,a}{(1-\nu^2)h}\left\{\frac{1}{2}\int_{-1}^{+1}\int_{-1}^{+1} G(X,T)\sigma(X)\sigma(T)dXdT\right.$$

$$\left. - \sigma_\infty \int_{-1}^{+1}\sqrt{1-X^2}\,\sigma(X)dX\right\}$$

$$+ \frac{2\,a}{3(3+\nu)(1-\nu)h}\left\{\frac{1}{2}\int_{-1}^{+1}\int_{-1}^{+1} G(X,T)m(X)m(T)dXdT\right.$$

$$\left. - m_\infty \int_{-1}^{+1}\sqrt{1-X^2}\,m(X)dX\right\}. \qquad (31)$$

Indeed, Ω may be shown to be the complementary energy of the plate and continuously distributed spring, apart from a multiplicative constant and a divergent additive term which does not depend on σ or m. Thus, the variational principle is just the complementary energy principle, but employed in such a way that we have used full solutions of the plane stress and plate bending equations to reckon the energy stored at material points away from the discontinuity in terms of the values of σ and m along the discontinuity. Of course, the first integral represents the energy of the continuously distributed spring.

Solution for a Special Case and Simple Approximation

It may be shown that

$$\int_{-1}^{+1} G(X,T)dT = \sqrt{1 - X^2} \quad . \tag{32}$$

Thus, if each of the dimensionless compliance coefficients varied in the form

$$\alpha_{\lambda\mu}(X) = \alpha^{o}_{\lambda\mu} \sqrt{1 - X^2} \quad , \quad \text{where } \alpha^{o}_{\lambda\mu} = \text{constant}, \tag{33}$$

then the solution of the integral equations is clearly that σ and m are constants given by

$$\frac{1 - \nu^2}{2} \frac{h}{a} [\alpha^{o}_{tt}\sigma + \alpha^{o}_{tb}m] + \sigma = \sigma_{\infty}$$

$$\frac{3(3 + \nu)(1 - \nu)}{2} \frac{h}{a} [\alpha^{o}_{bt}\sigma + \alpha^{o}_{bb}m] + m = m_{\infty} \tag{34}$$

The solution is

$$0\sigma = \left[1 + \frac{3(3 + \nu)(1 - \nu)}{2} \frac{h}{a} \alpha^{o}_{bb}\right] \sigma_{\infty} - \frac{1 - \nu^2}{2} \frac{h}{a} \alpha^{o}_{tb} m_{\infty}$$

$$0m = - \frac{3(3 + \nu)(1 - \nu)}{2} \frac{h}{a} \alpha^{o}_{bt}\sigma_{\infty} + \left[1 + \frac{1 - \nu^2}{2} \frac{h}{a} \alpha^{o}_{tt}\right] m_{\infty} \tag{35}$$

where

$$0 = \left[1 + \frac{1 - \nu^2}{2} \frac{h}{a} \alpha^o_{tt}\right] \left[1 + \frac{3(3 + \nu)(1 - \nu)}{2} \frac{h}{a} \alpha^o_{bb}\right]$$

$$- \frac{3(3 + \nu)(1 - \nu)(1 - \nu^2)}{4} \left(\frac{h}{a}\right)^2 \left(\alpha^o_{tb}\right)^2 \qquad (36)$$

In general, no shape of a crack exists which is consistent with the assumed functional form of eq. (33) for the compliance coefficients. [An exception is the case of a very shallow crack, $\ell/h << 1$, having depth ℓ proportional to $(1 - X^2)^{1/4}$]. However, the approximation so much reduces the complexity of the problem that it is well worth examination. Two methods for the choice of $\alpha^o_{\lambda\mu}$ suggest themselves. The simplest is to identify $\alpha^o_{\lambda\mu}$ with the value of $\alpha_{\lambda\mu}(X)$ at $X = 0$,

$$\alpha^o_{\lambda\mu} = \alpha_{\lambda\mu}(0) \qquad (37)$$

A slightly more complicated method is to choose $\alpha^o_{\lambda\mu}$ so that both sides of eq. (33) agree in an integrated average along the length of the discontinuity, and this gives

$$\alpha^o_{\lambda\mu} = \frac{2}{\pi} \int_{-1}^{+1} \alpha_{\lambda\mu}(X)dX \qquad (38)$$

In fact, this latter method of choosing $\alpha^o_{\lambda\mu}$ is suggested by quite different considerations: Let us make no assumptions about the variation of $\alpha_{\lambda\mu}$ with X. Rather, consider the variational formulation of the problem, as in the last section, and let us minimize Ω on the class of functions σ = constant and m = constant along the discontinuity. It may be seen that

σ and m then satisfy eqs. (34), so that the solution is as in eqs. (35), provided that the symbols $\alpha^{o}_{\lambda\mu}$ are defined just as in eq. (38). We shall compare this simple approximation with numerical solutions of the integral equations, as discussed below.

Numerical Solution of the Integral Equations

A numerical formulation is developed here for the case in which the part-through crack is semi-elliptical in shape,

$$\left[\frac{\ell(x_1)}{\ell_o}\right]^2 + \left(\frac{x_1}{a}\right)^2 = 1 \ , \quad \text{or} \quad \ell(x_1) = \ell_o(1-X^2)^{1/2} \tag{39}$$

The compliance coefficients are therefore, from eqs. (15),

$$\alpha_{\lambda\mu}(X) = \left(\frac{\ell_o}{h}\right)^2 (1-X^2) \sum_{n=0}^{8} C^{(n)}_{\lambda\mu} \left(\frac{\ell_o}{h}\right)^n (1-X^2)^{n/2} \tag{40}$$

From symmetry, $\sigma(X)$ and $m(X)$ need only be determined in the interval $0 \leq X \leq 1$. This is done as follows: Referring to fig. 5, we divide the interval into a number of subdivisions (fourteen in the figure), and represent $\sigma(X)$ and $m(X)$ as piecewise linear functions. The unknowns are then the values of σ and m at the nodes (i.e., at X=0, 1/8, 1/4,...,30/32, 31/32,1). We choose these values so that the integral eqs. (30) are satisfied exactly at each node. Thus, if there are n subdivisions so that the nodes are at X_o=0 , X_1 , X_2 ,..., X_n=1 , with σ_0 ,..., σ_n and m_0 ,..., m_n being the corresponding values of σ and m , then the discretized form of the first of the integral eqs. (30) is

$$\frac{1-\nu^2}{2}\,\frac{h}{a}\,[\alpha_{tt}(X_k)\sigma_k + \alpha_{tb}(X_k)m_k] + \sum_{j=1}^{n}\int_{X_{j-1}}^{X_j}[G(X_k,X)$$

$$+ G(X_k,-X)]\,[\sigma_{j-1} + (\sigma_j-\sigma_{j-1})(X-X_{j-1}) \,/\, (X_j-X_{j-1})]dX$$

$$= \sigma_\infty\sqrt{1-X_k^2}\quad,\qquad \text{for } k=0,\,1,\,2,\ldots,\,n\,. \tag{41}$$

and a similar form applies for the second integral equation. The integrations were done by standard numerical routines, except for those intervals where $G(X_k,X)$ is singular. In these intervals the singular part of the kernel, $\log|X_k-X|$, was separated out and integrated in closed form, whereas the remainder of the kernel was integrated numerically. A special interpretation must be made of eq. (41) for $k=n$ (i.e., at the end of the interval, $X_k=1$). This is because $\alpha_{\lambda\mu}(1)$ and $G(1,X)$ are zero, as is also the right side of the equation. We are left with $0=0$. The proper form of eqs. (30) at $X=1$ results by dividing both sides by $(1-X^2)^{1/2}$ and letting $X\to1$. Thus, Since

$$\lim_{X\to1}\frac{\alpha_{\lambda\mu}(X)}{(1-X^2)^{1/2}} = 0\,,\quad\text{and}\quad \lim_{X\to1}\frac{G(X,T)}{(1-X^2)^{1/2}} = \frac{1}{\pi}\left(\frac{1+T}{1-T}\right)^{1/2}\,, \tag{42}$$

we have

$$\frac{1}{\pi}\int_{-1}^{+1}\left(\frac{1+T}{1-T}\right)^{1/2}\begin{Bmatrix}\sigma(T)\\ m(T)\end{Bmatrix}dT = \begin{Bmatrix}\sigma_\infty\\ m_\infty\end{Bmatrix}\,. \tag{43}$$

Thus, the discretized equation which replaces eq. (41) when $k=n$ is

$$\frac{2}{\pi} \sum_{j=1}^{n} \int_{X_{j-1}}^{X_j} (1-X^2)^{-1/2} \left[\sigma_{j-1} + (\sigma_j-\sigma_{j-1})(X-X_{j-1}) \Big/ (X_j-X_{j-1})\right] dX = \sigma_\infty \, . \tag{44}$$

The condition expressed by eq. (43) has a simple interpretation: Looking back to eqs. (21,24) for the complex potentials, $\phi_t(z)$ and $\phi_b(z)$, we see that eq. (43) is the condition for those potentials to remain bounded at the ends of the line of discontinuity. Hence the thickness average stresses $\sigma_{\alpha\beta}$ and moments $m_{\alpha\beta}$ will be bounded at the ends of the line of discontinuity. In fact, this same conclusion may be shown to follow if the depth of the part through crack approaches zero at the ends as

$$\ell(x_1) \to (1-X^2)^q \text{ times term of order unity at } X = \pm 1 \, ,$$

where q is any positive number exceeding $1/4$.

Results

Results presented in figs. 6 to 10, from numerical solution of the integral equations, are based on the 14 spacings (and thus 30 unknown nodal values) shown in fig. 5. The finer subdivisions were employed near the ends since preliminary solutions revealed large gradients in σ and m there. Doubling the number of subdivisions makes for less than 1% difference in results for σ_0 and m_0 (from which we compute the stress intensity factor at the crack midpoint $x_1 = 0$), although values of σ_n and m_n change by as much as 7

to 15%. Calculations were performed on the IBM 360/67 at Brown University. Two solutions were run for each geometric configuration studied, one for the case of a pure tensile load ($\sigma_\infty = 1$, $m_\infty = 0$) and one for a pure bending load ($\sigma_\infty = 0$, $m_\infty = 1$) .

According to eq. (6), the stress intensity factor at the crack midpoint is given in terms of σ_0 and m_0 by

$$K = h^{1/2} [\sigma_0 g_t + m_0 g_b] \quad ,$$

g_t and g_b being evaluated for the midpoint depth ratio, ℓ_o/h . In presenting numerical results we make K dimensionless through division by K_∞ , the stress intensity factor of the edge crack in plane strain for the same ℓ_o/h ratio and remote tensile or bending load. This is, of course, the limiting value of K for the part-through crack as the surface length becomes infinite.

Fig. 6 shows K/K_∞ for a pure tensile load, as a function of the dimensionless crack depth (ℓ_o/h) and surface length ($2a/h$); fig. 7 presents the same for a pure bending load. One notable feature of the results is that a very large surface length is necessary (for moderate to deep crack depths) for the part-through crack stress intensity factor to approach that of the plane strain edge crack in a strip. Evidently, the part-through crack causes substantial load shedding to uncracked regions of the plate, as a consequence of the localized increase in elastic compliance at the cracked section.

Fig. 8 shows the comparison between K as obtained from the numerical solution of the integral equations (solid lines) and from the simple approximation for

σ and m of eqs. (35,38) (dashed lines). This figure is for the pure tensile load case. Similar but slightly smaller discrepancies result between the two in the pure bending case. Thus, while the errors of the approximation are not small, its use may be recommended both for its simplicity and for its giving a conservative overestimate to the intensity factor.

Fig. 9 shows the variation of σ and m with distance from the crack midpoint for the case of a pure tensile load. These results are for $\ell_o/h = 1/2$, and for several values of $2a/h$. Fig. 10 shows the same for a pure bending load. It is interesting to note that the pure bending load induces little nominal tensile stress on the cracked section, while the pure tensile load induces a significant nominal bending stress. Values of σ and m at $X = 1$ indicate (in a thickness averaged sense) the severity of the stress concentration at the ends of the part-through cracked section.

Our use of the two-dimensional plane stress and plate bending theories is based on the assumption that the surface length of the crack exceeds, say, two or more plate thicknesses. Smith et al. [8] have treated the part-through crack problem making use of approximate solutions of the three-dimensional elastic field equations, and gave results for cracks with $2a/h \leq 1$. Their analysis modelled the semi-elliptical surface crack as a crack in the form of an arc of a circle, and was phrased in terms of correction factors, first suggested by Irwin [9], on the embedded elliptical crack solution [10] to account for: 1) the presence of the free surface through the crack plane, and 2) the finite thickness of the plate. Table 2 compares numerical results for K at the crack midpoint, as taken from Smith et al., with results from our calculations although, strictly speaking, all the $2a/h$ range shown is outside the range of validity of our model. Nevertheless,

the close agreement with the presumably more accurate calculations is striking. (Smith et al. discuss three methods of matching the arc of a circle to a semi-ellipse. Results in the table are based on matching curvature and depth at the crack midpoint, and fall between the other two methods of matching surface length or crack area in addition to midpoint depth.)

It is apparent that our model may readily be extended to part-through cracks in curved shell structures, resulting in analyses within the framework of two-dimensional shell theory. This is a great simplification, to be exploited in future work. Further, a similar model will allow treatment of part-through cracks in ductile plates or shells for which a segment of the part-cracked section is completely yielded. The simplest treatment would employ an elastic-perfectly plastic line spring, with results of plane strain plastic limit analyses for the strip of fig. 2 employed to obtain values of σ and m corresponding to yield.

Acknowledgment

Support of this study by the National Aeronautics and Space Administration, under Grant NGL-40-002-080, is gratefully acknowledged.

dwa

References

1) G. R. Irwin, "Fracture Mechanics", in Structural Mechanics, (J. N. Goodier and N. J. Hoff, Eds.), Pergamon Press, 1960, p. 557.

2) P. C. Paris and G. C. Sih, "Stress Analysis of Cracks", in Fracture Toughness Testing and its Applications, STP-381, ASTM, 1965, p. 30.

3) W. T. Koiter, Discussion of "Rectangular Tensile Sheet with Symmetric Edge Cracks" by O. L. Bowie, ASME J. Appl. Mech., vol. 32, 1965, p. 237.

4) B. Gross and J. E. Srawley, "Stress Intensity Factors for Single Edge Notch Specimens in Bending or Combined Bending and Tension by Boundary Collocation of a Stress Function", NASA Tech. Note D-2603, 1965.

5) H. Okamura, H. W. Liu, C. S. Chu, and H. Liebowitz, "A Cracked Column Under Compression", Engr. Fracture Mech., vol. 1, 1969, p. 547.

6) N. I. Muskhelishvili, Some Basic Problems in the Mathematical Theory of Elasticity (J. R. M. Radok, trans.), Noordhoff, Groningen, 1953.

7) G. N. Savin, Stress Concentration Around Holes (E. Gros, trans.; W. Johnson, ed.), Pergamon Press, 1961.

8) F. W. Smith and M. J. Alavi, "Stress-Intensity Factors for a Part-Circular Surface Flaw", ASME, Proceedings of the First International Conference on Pressure Vessel Technology, 1969.

9) G. R. Irwin, "Crack Extension Force for a Part Through Crack in a Plate", ASME J. Appl. Mech., Vol. 29, 1962, p. 651.

10) A. E. Green and I. N. Sneddon, "The Distribution of Stress in the Neighborhood of a Flat Elliptic Crack in an Elastic Solid:, Proceedings of the Cambridge Philosophical Society, Vol. 46, 1950, pp. 159-163.

Appendix: Use of relation between K and variation of potential energy with crack depth, and its equivalence to the method adopted earlier.

The potential energy of a finite (later, replace finite by infinite) plate, of the sort in fig. 3 with a continuously distributed spring representing a partially through the thickness crack, is

$$P = \frac{h}{2}\int_{\substack{\text{area of}\\ \text{plate}}} [\sigma_{\alpha\beta}\frac{\partial u_\alpha}{\partial x_\beta} + \frac{h}{6}m_{\alpha\beta}\frac{\partial^2 u_3}{\partial x_\alpha \partial x_\beta}]\,dx_1dx_2$$

$$+ \frac{h}{2}\int_{-a}^{+a} [\sigma\delta + \frac{h}{6}m\theta]dx_1$$

$$- \int_{\text{boundary}} [N_\alpha u_\alpha + M_\alpha \frac{\partial u_3}{\partial x_\alpha}]ds, \qquad (A1)$$

where α,β range over 1, 2, where N_α and M_α are the boundary force and moment per unit length of middle surface, and s is arc length around the boundary. Clearly, the first integral gives the strain energy of the stretching and bending fields, the second integral gives the strain energy of the line spring, and the last integral gives the potential energy of the boundary load system. Let $\sigma_{\alpha\beta}$, u_3, δ, m, etc. represent the solution when the crack depth is $\ell(x_1)$, and let $\sigma_{\alpha\beta} + \Delta\sigma_{\alpha\beta}$, $u_3 + \Delta u_3$, $\delta + \Delta\delta$, $m + \Delta m$, etc. represent the solution when the crack depth is $\ell(x_1) + \Delta\ell(x_1)$, the boundary loads being the same in both cases. The associated change in potential energy is, to first order in the Δ quantities.

$$\Delta P = \frac{h}{2} \int_{\substack{\text{area of}\\ \text{plate}}} [(\Delta\sigma_{\alpha\beta} \frac{\partial u_\alpha}{\partial x_\beta} + \sigma_{\alpha\beta} \frac{\partial \Delta u_\alpha}{\partial x_\beta}) + \frac{h}{6} (\Delta m_{\alpha\beta} \frac{\partial^2 u_3}{\partial x_\alpha \partial x_\beta}$$

$$+ m_{\alpha\beta} \frac{\partial^2 \Delta u_3}{\partial x_\alpha \partial x_\beta})] dx_1 dx_2$$

$$+ \frac{h}{2} \int_{-a}^{+a} [(\Delta\sigma\delta + \sigma\Delta\delta) + \frac{h}{6} (\Delta m\theta + m\Delta\theta)] dx_1$$

$$- \int_{\text{boundary}} [N_\alpha \Delta u_\alpha + M_\alpha \frac{\partial \Delta u_3}{\partial x_\alpha}] ds \qquad \text{(A-2)}$$

We know that the potential energy change may be related to Irwin's energy release rate, G , b,

$$-\Delta P = \int_{\substack{\text{crack}\\ \text{tip}}} G\Delta\eta ds \qquad \text{(A-3)}$$

where s is arc length along the crack tip, $\Delta\eta$ is the advance of the crack normal to itself, and where the formula is correct to first order in $\Delta\eta$. But to first order, $\Delta\eta ds = \Delta\ell dx_1$, and

$$-\Delta P = \int_{-a}^{+a} G\Delta\ell \, dx_1 \, . \qquad \text{(A-4)}$$

Hence, if we compute ΔP from eq. (A-2) for arbitrary $\Delta\ell(x_1)$, we will have an estimate of G (or K) at points along the crack tip. In fact, we shall see that this method gives a result for K which is identical to that of the method employed in the paper, in which we related χ to the force and

moment along the discontinuity through the plane strain result of eq. (6).

We shall employ the principle of virtual work, adapted to the plate with a line of discontinuity, to write

$$\int_{\text{boundary}} (N_\alpha \Delta u_\alpha + M_\alpha \frac{\partial \Delta u_3}{\partial x_\alpha}) ds$$

$$= h \int_{\substack{\text{area of} \\ \text{plate}}} [\sigma_{\alpha\beta} \frac{\partial \Delta u_\alpha}{\partial x_\beta} + \frac{h}{6} m_{\alpha\beta} \frac{\partial^2 \Delta u_3}{\partial x_\alpha \partial x_\beta}] dx_1 dx_2$$

$$+ h \int_{-a}^{+a} [\sigma \Delta\delta + \frac{h}{6} m \Delta\theta] dx_1 \ . \qquad \text{(A-5)}$$

This modifies eq. (A-2) to

$$P = \frac{h}{2} \int_{\substack{\text{area of} \\ \text{plate}}} [(\Delta\sigma_{\alpha\beta} \frac{\partial u_\alpha}{\partial x_\beta} - \sigma_{\alpha\beta} \frac{\partial \Delta u_\alpha}{\partial x_\beta}) + \frac{h}{6} (\Delta m_{\alpha\beta} \frac{\partial^2 u_3}{\partial x_\alpha \partial x_\beta} - m_{\alpha\beta} \frac{\partial^2 \Delta u_3}{\partial x_\alpha \partial x_\beta})] dx_1 dx_2$$

$$+ \frac{h}{2} \int_{-a}^{+a} [(\Delta\sigma\delta - \sigma\Delta\delta) + \frac{h}{6} (\Delta m\theta - m\Delta\theta) dx_1 \qquad \text{(A-6)}$$

The area integral vanishes by elastic reciprocity, and we are left with

$$-\Delta P = \frac{h}{2} \int_{-a}^{+a} [(\sigma\Delta\delta - \Delta\sigma\delta) + \frac{h}{6} (m\Delta\theta - \Delta m\theta) dx_1 \qquad \text{(A-7)}$$

At this point it will cause no difficulty if the plate is considered to be infinite.

By relating δ and θ to σ and m by eq. (9), we may write

$$h(\sigma\Delta\delta - \Delta\sigma\delta) = \sigma\Delta(A_{tt}\sigma + A_{tb}m) - \Delta\sigma(A_{tt}\sigma + A_{tb}m)$$

$$= \sigma\left(\frac{dA_{tt}}{d\ell}\sigma + \frac{dA_{tb}}{d\ell}m\right)\Delta\ell + \sigma(A_{tt}\Delta\sigma + A_{tb}\Delta m) - \Delta\sigma(A_{tt}\sigma + A_{tb}m) \qquad \text{(A-8)}$$

and a similar formula for

$$\frac{h^2}{6}\,(m\Delta\theta - \Delta m\theta)\,,$$

so that eq. (A-7) for ΔP becomes

$$-\Delta P = \int_{-a}^{+a} \left\{\frac{1}{2}\left[\sigma\left(\frac{dA_{tt}}{d\ell}\sigma + \frac{dA_{tb}}{d\ell}m\right) + m\left(\frac{dA_{bt}}{d\ell}\sigma + \frac{dA_{bb}}{d\ell}m\right)\right]\right\} \Delta\ell\, dx_1. \qquad \text{(A-9)}$$

Upon conparing this to eq. (A-4), we can see that G must be set equal to the quantity in $\{...\}$, in equation (A-9), if we are to estimate G from the variation in potential energy. But looking back to eq.(11) and (12), we see that the derivatives of the compliance coefficients have been defined such that the quantity in $\{...\}$ is simply the value for G which results when the stress intensity factor is written as in eq. (6) for the plane strain problem. Thus, we see that the method adopted in the paper, for relating K to the force and moment acting on the line of discontinuity, is entirely equivalent to a method based on the relation between K and the potential energy variation with respect to crack depth.

n	$c_{tt}^{(n)}$	$c_{tb}^{(n)}$	$c_{bb}^{(n)}$
0	1.98	1.98	1.98
1	-0.54	-1.91	-3.28
2	18.65	16.01	14.43
3	-33.70	-34.84	-31.26
4	99.26	83.93	63.56
5	-211.90	-153.65	-103.36
6	436.84	256.72	147.52
7	-460.48	-244.67	-127.69
8	289.98	133.55	61.50

TABLE 1: Coefficients in the power series of eqs. (15) for the dimensionless compliances α_{tt}, α_{tb}, α_{bb}.

ℓ_o/h	2a/h	$K/(h^{1/2}\sigma_\infty)$ present paper	$K/(h^{1/2}\sigma_\infty)$ Smith et al. [8]
0.1	0.25	0.41	0.42
0.2	0.4	0.48	0.51
0.2	0.5	0.52	0.60
0.3	0.6	0.57	0.63
0.3	0.75	0.63	0.73
0.4	0.8	0.68	0.70
0.4	1.0	0.76	0.84
0.5	1.0	0.82	0.82
0.5	1.25	0.90	0.94
0.6	1.2	0.96	0.91
0.6	1.5	1.06	1.15

TABLE 2: Stress-intensity factors at mid-point of semi-elliptic crack under pure tensile loading: comparison with ref. [8].

Figure Captions

1. A surface crack penetrating part-through the thickness of a plate loaded in tension and bending.

2. Plane strain of an edge cracked strip subjected to thickness average tensile stress $\sigma(= N/h)$ and nominal bending stress $m(= 6M/h^2)$.

3. Two-dimensional plane stress-plate bending model with line spring representing part-through crack of fig. 1. Compliance coefficients at points along the line spring are matched to those of the edge cracked strip in plane strain, fig. 2.

4. a) Stress intensity factor coefficients g_t (for tensile load) and g_b (for bending load), for edge cracked strip of fig. 2, as a function of crack depth to thickness ratio ℓ/h (see eq. 6).

   b) Dimensionless compliance coefficients $\alpha_{\lambda\mu}$ (see eq. 13) for additional extension δ and rotation θ of strip due to introduction of crack. These are employed as compliance coefficients for the line spring of fig. 3.

5. For numerical solution of the integral equations, the nominal tensile and bending stresses on the part-through cracked section are represented as piecewise linear functions determined by the unknown values of σ and m at the "nodes".

6. Stress intensity factor at midpoint of the part-through crack, for pure tensile load σ_∞ on plate of fig. 1 (i.e., $m_\infty = 0$). The crack is assumed to be semi-elliptical in shape, with depth ℓ_o at its midpoint and surface length $2a$. The stress intensity factor is made dimensionless through division by its value for $a \to \infty$ (corresponding to edge crack of depth ℓ_o in a strip under plane strain).

7. Same as fig. 6, but for pure <u>bending</u> load m_∞ on plate of fig. 1 (i.e., $\sigma_\infty = 0$).

8. Comparison of stress intensity factor at midpoint of crack, for pure tensile load, as computed from numerical solution of integral equations (solid lines, from fig. 6) and from simple approximation based on eqs. (35,38) (dashed lines). Similar but slightly smaller discrepancies result for pure bending load.

9. Nominal stresses acting on part-through cracked section, as a function of distance from midpoint, for pure tensile load on plate of fig. 1. Calculations for midpoint crack depth of half the plate thickness, and for various values of 2a/h. Solid lines represent results of the numerical calculations, whereas the dashed lines are from the simple approximation of eqs. (35,38). (a) Nominal tensile stress σ/m_∞. (b) Nominal bending stress m/σ_∞.

10. Same as fig. 9, but for pure bending load (a) Nominal tensile stress σ/m_∞. (b) Nominal bending stress m/m_∞.

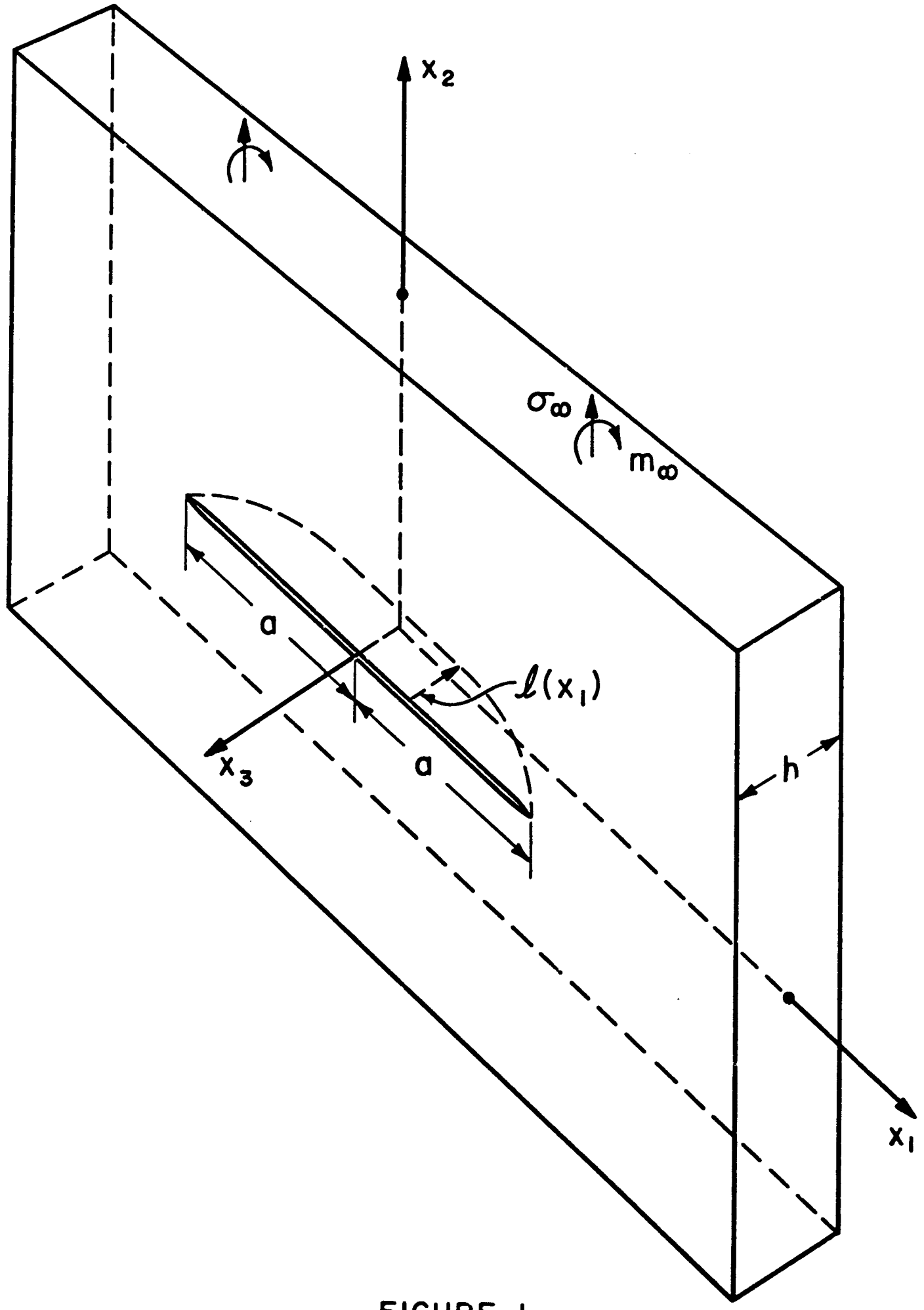

FIGURE 1

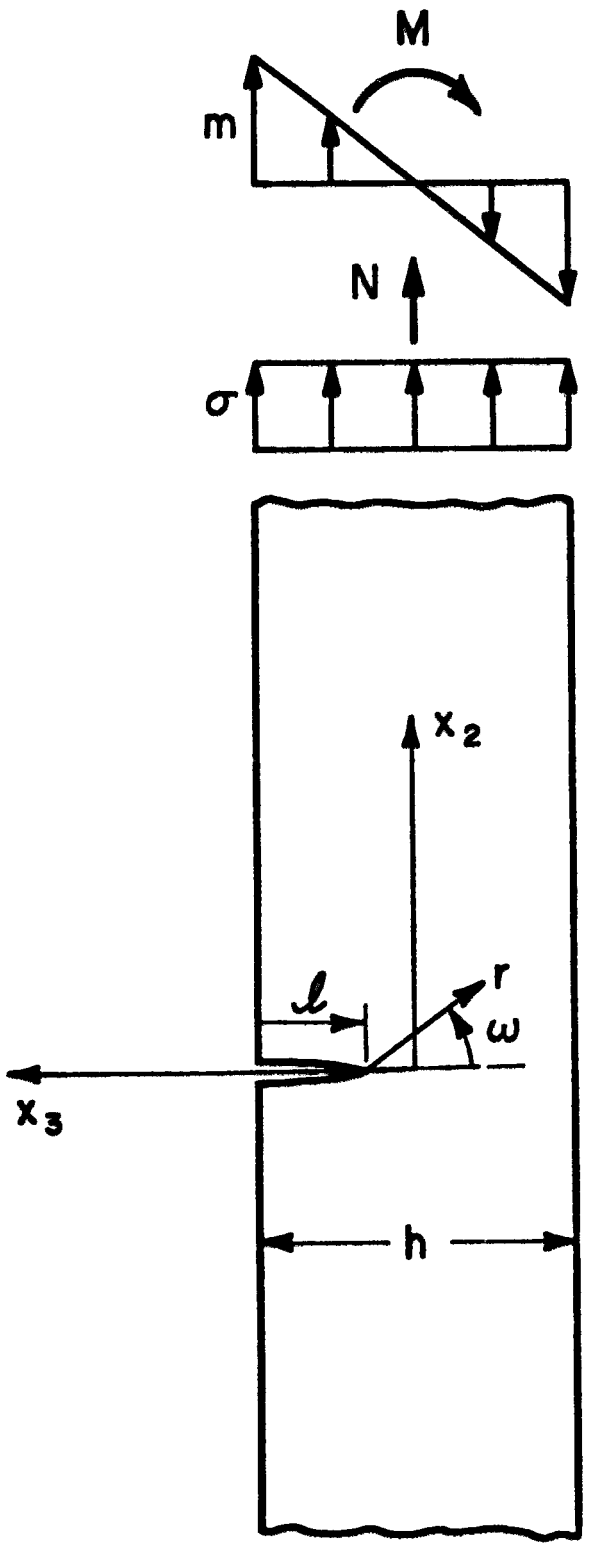

FIGURE 2

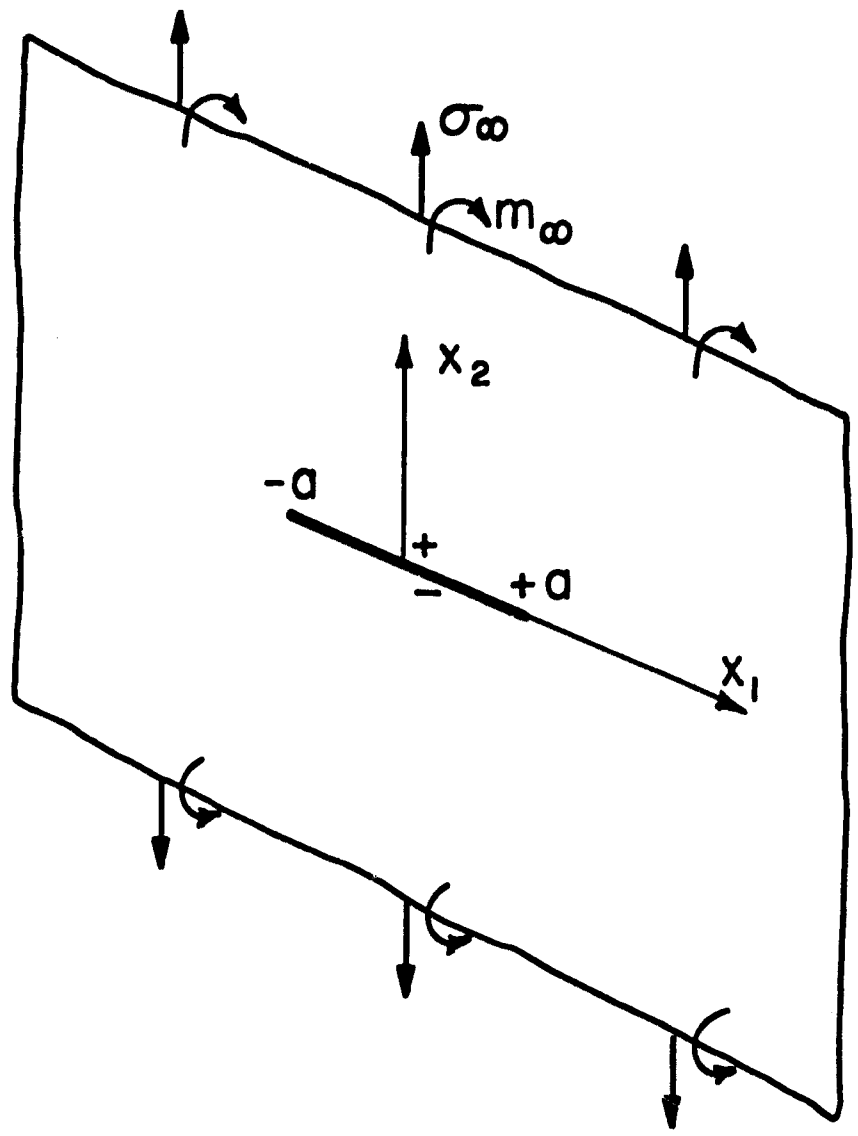

FIGURE 3

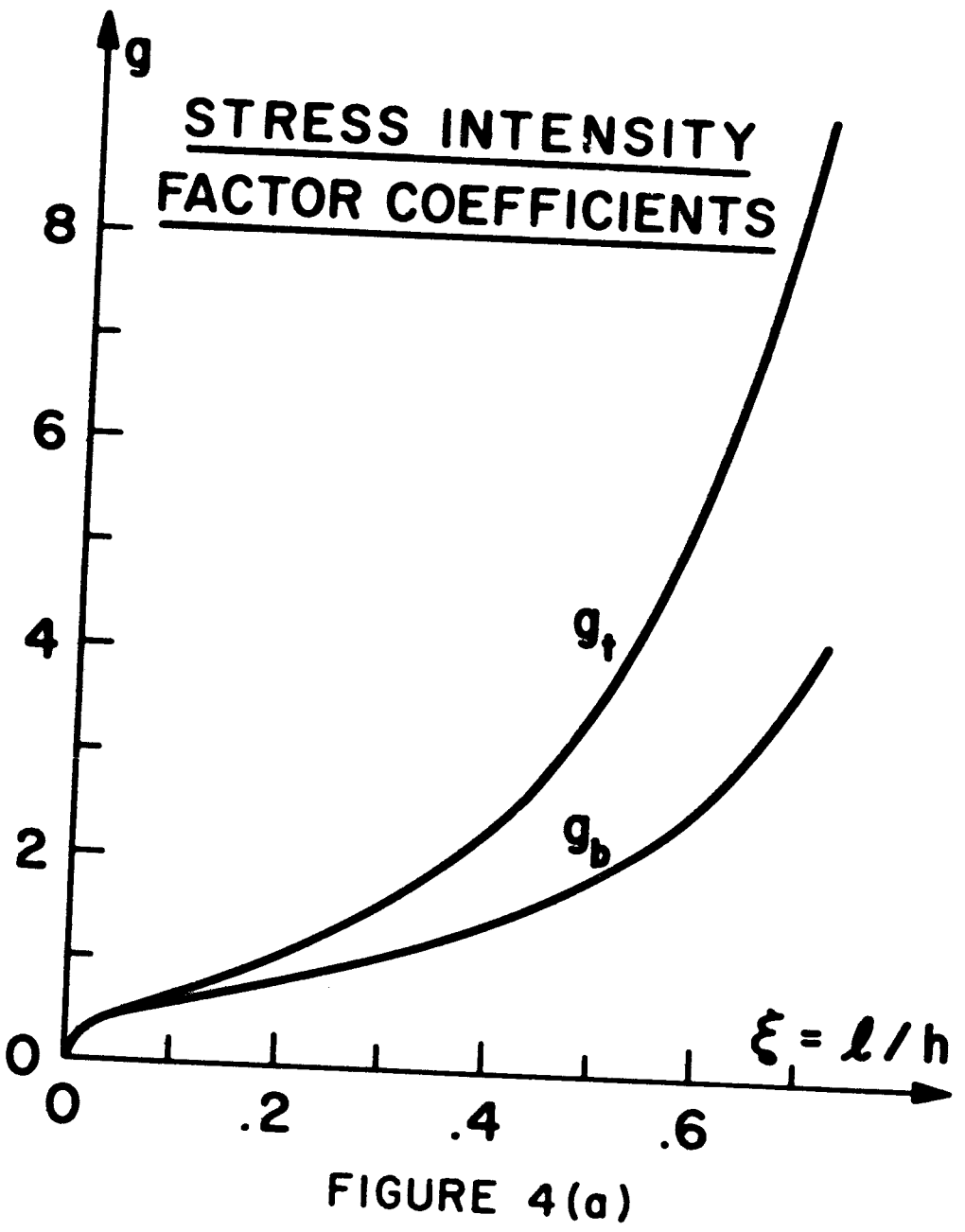

FIGURE 4(a)

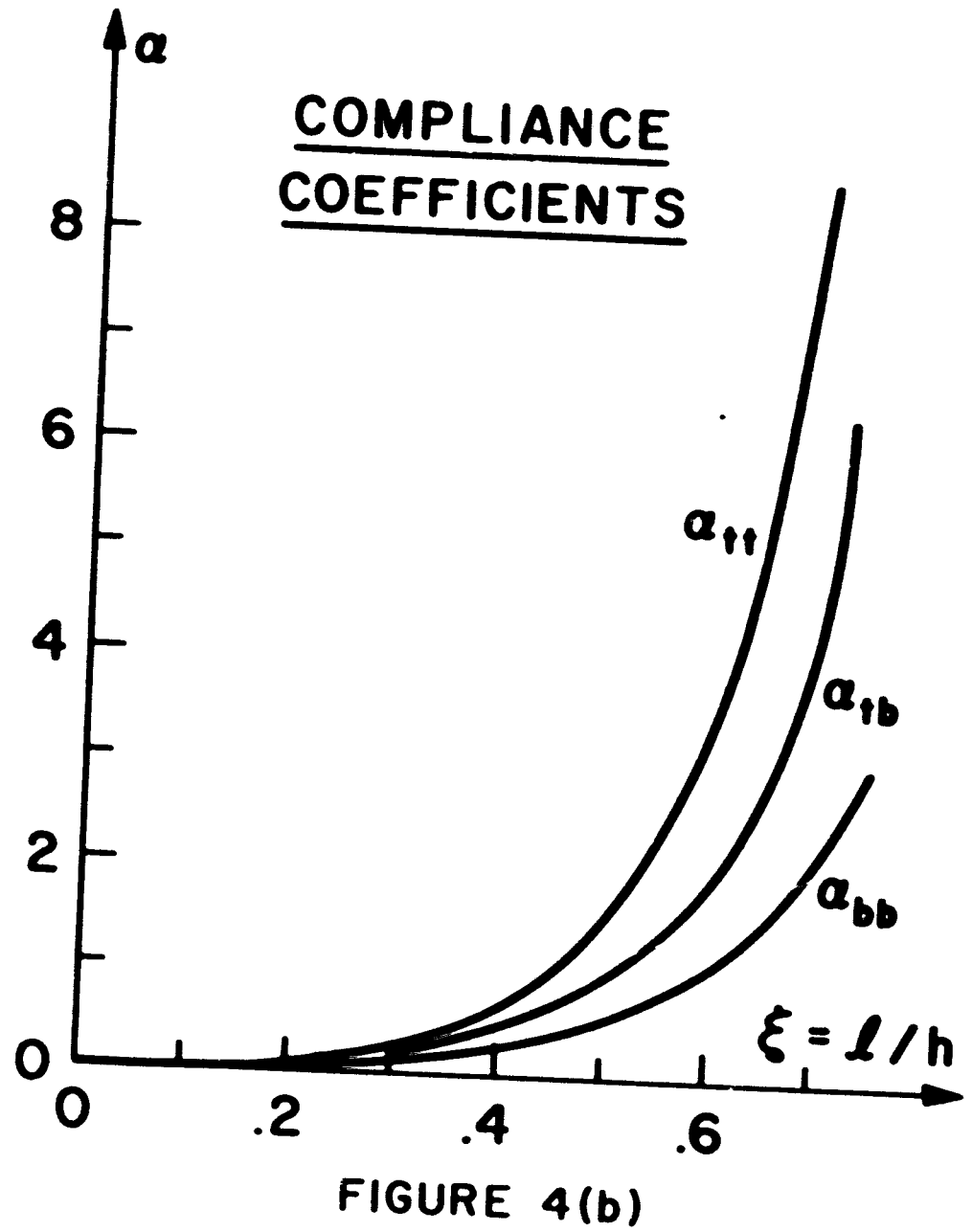

FIGURE 4(b)

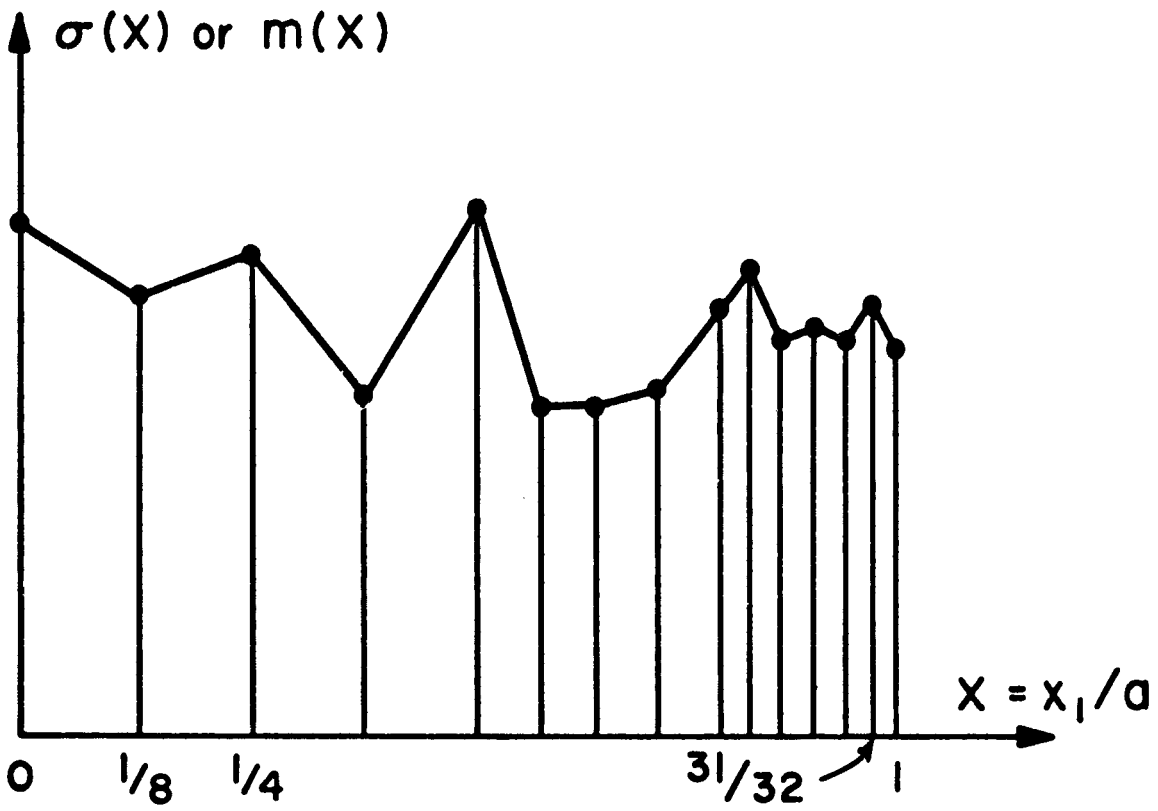

FIGURE 5

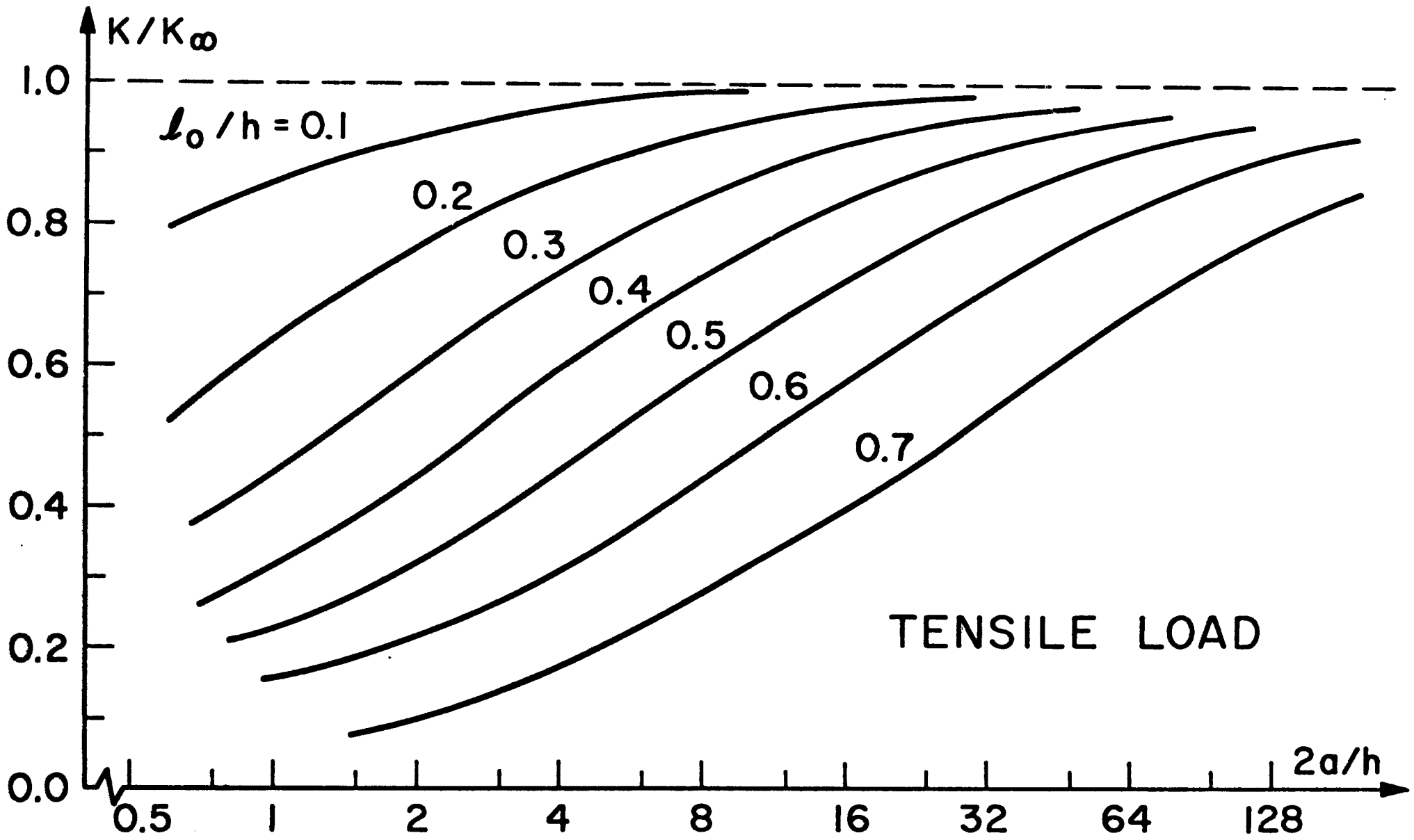
K/K∞
1.0
0.8
0.6
0.4
0.2
0.0
ℓ₀/h = 0.1
0.2
0.3
0.4
0.5
0.6
0.7
TENSILE LOAD
2a/h
0.5
1
2
4
8
16
32
64
128

FIGURE 6

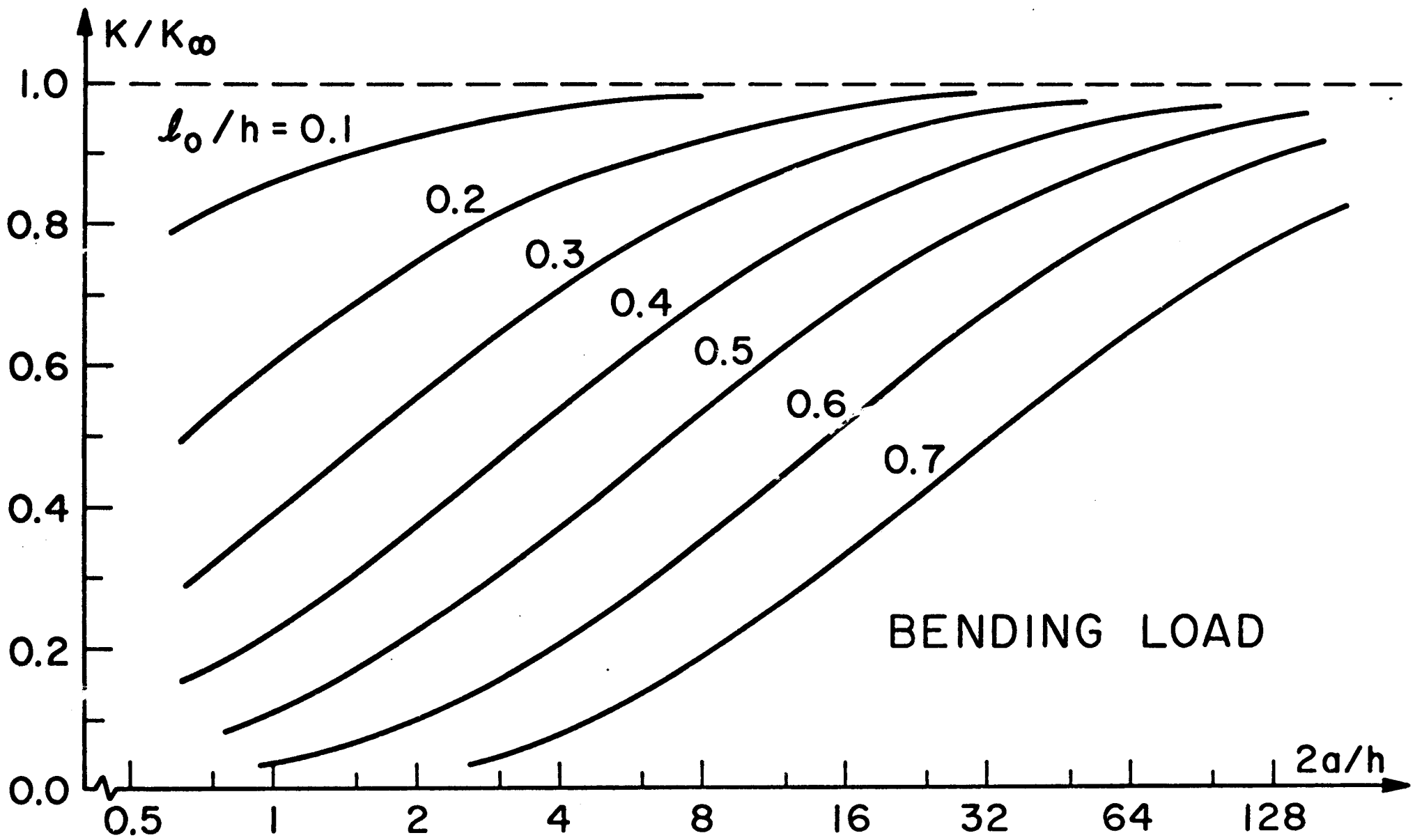
K/K∞
1.0
0.8
0.6
0.4
0.2
0.0
ℓ0/h = 0.1
0.2
0.3
0.4
0.5
0.6
0.7
BENDING LOAD
2a/h
0.5
1
2
4
8
16
32
64
128

FIGURE 7

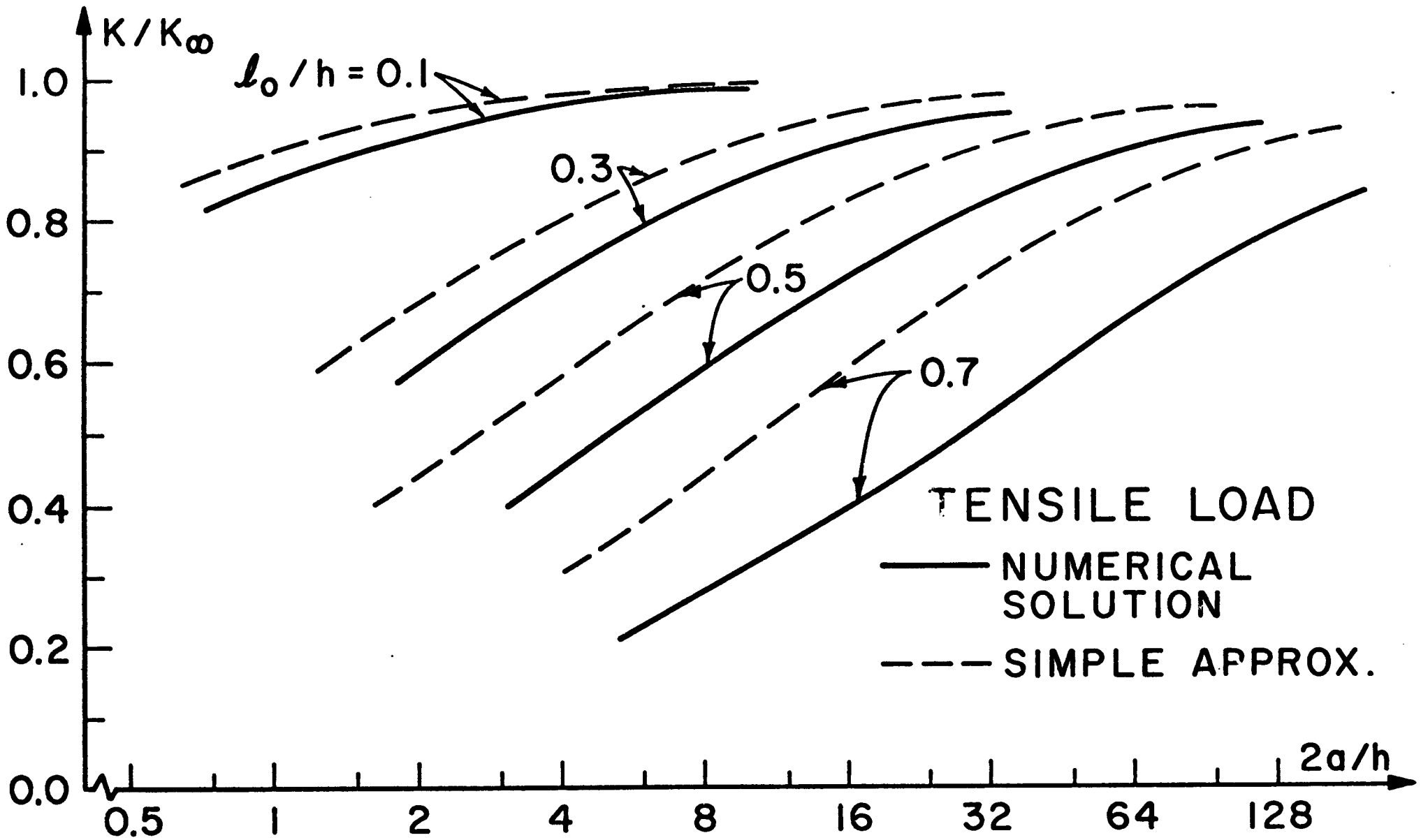
K / K∞
1.0
0.8
0.6
0.4
0.2
0.0
ℓ₀ / h = 0.1
0.3
0.5
0.7
TENSILE LOAD
NUMERICAL SOLUTION
SIMPLE APPROX.
2a/h
0.5
1
2
4
8
16
32
64
128

FIGURE 8

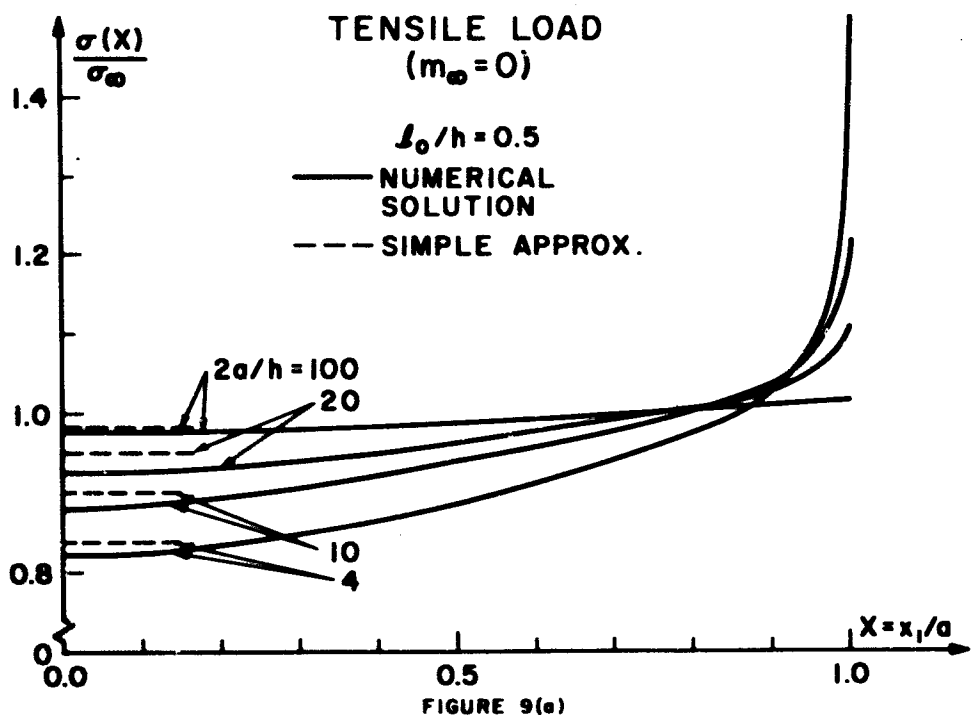

FIGURE 9(a)

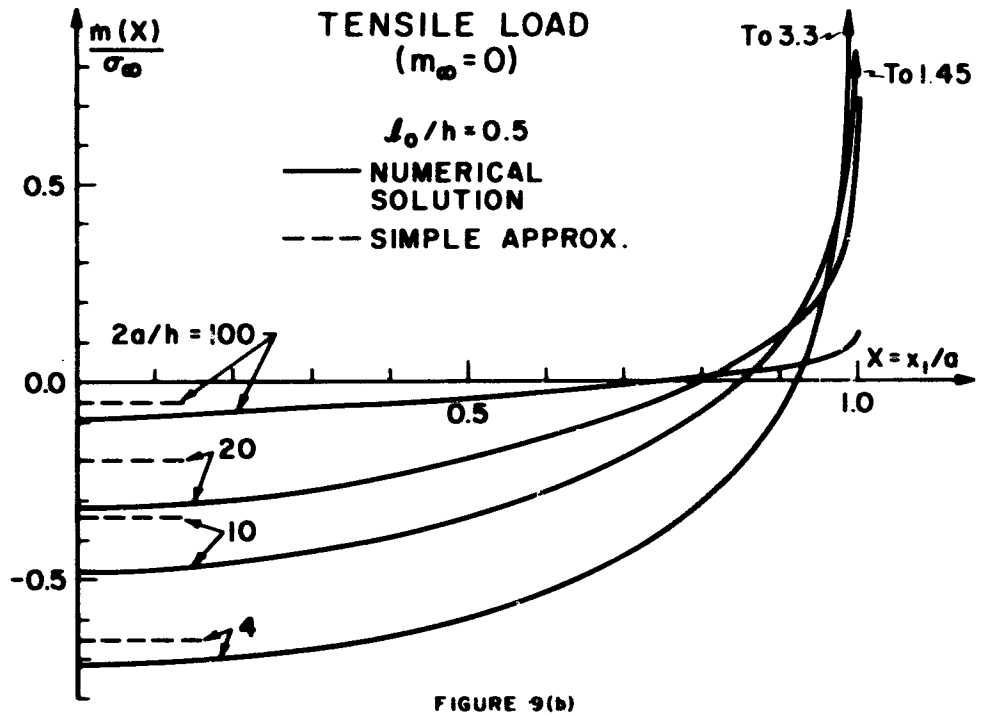

FIGURE 9(b)

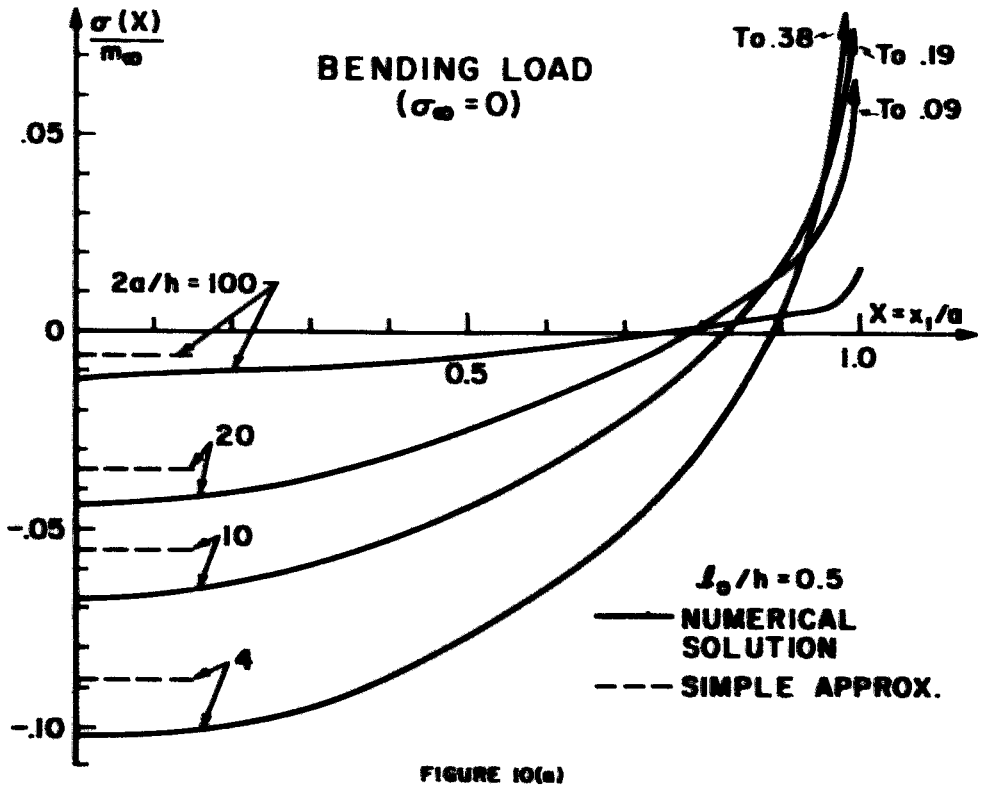

FIGURE 10(a)

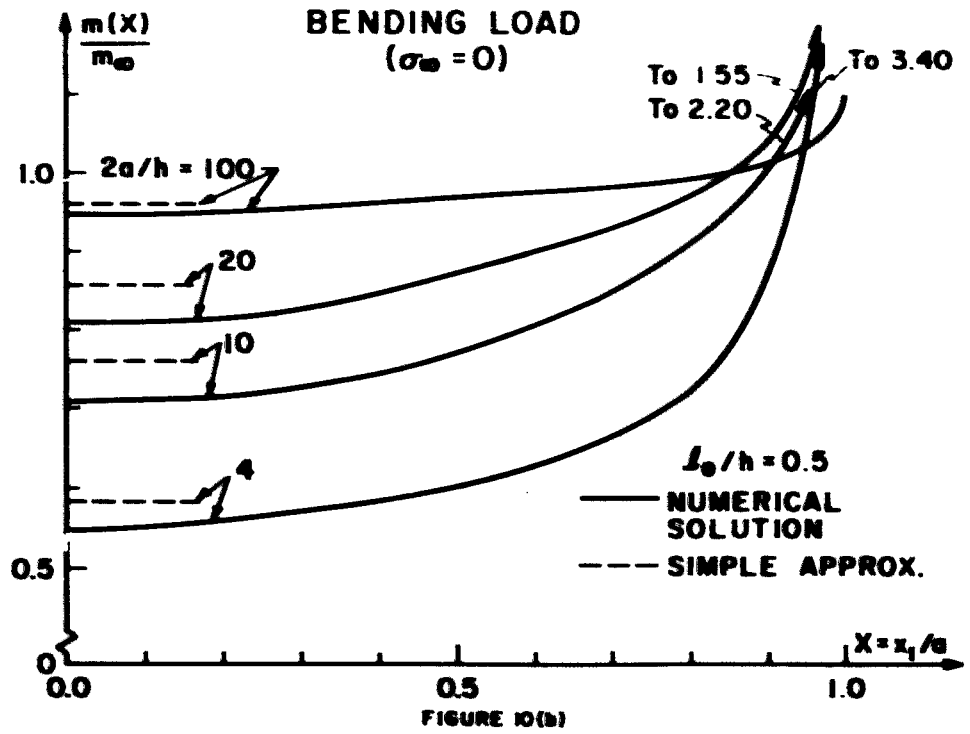

FIGURE 10(b)